Computers & Fluids 72 (2013) 46–62

Contents lists available at SciVerse ScienceDirect

Computers & Fluids

journal homepage: www.elsevier.com/locate/compfluid

MHD natural convection and entropy generation in a trapezoidal enclosure using Cu–water nanofluid

Amir Houshang Mahmoudi [a,b], Ioan Pop [c,*], Mina Shahi [a,d], Farhad Talebi [a]

[a] Faculty of Mechanical Engineering, Semnan University, Semnan, Iran
[b] Faculty of Science, Technology and Communication (FSTC), University of Luxembourg, Luxembourg
[c] Department of Mathematics, Babeş-Bolyai University, 400084 Cluj-Napoca, Romania
[d] Laboratory of Thermal Engineering, Faculty of Engineering Technology, University of Twente, Enschede, The Netherlands

ARTICLE INFO

Article history:
Received 4 May 2012
Received in revised form 23 September 2012
Accepted 27 November 2012
Available online 12 December 2012

Keywords:
Nanofluid
MHD
Natural convection
Numerical study
Entropy generation
Trapezoidal enclosure

ABSTRACT

The present work investigates the entropy generation and enhancement of heat transfer in natural convection flow and heat transfer using Copper (Cu)–water nanofluid in the presence of a constant magnetic field. The analysis uses a two dimensional trapezoidal enclosure with the left vertical wall and inclined walls kept in a low constant temperature and a heat source with constant heat flux placed on the bottom wall of the enclosure. The governing equations were discretized by the control volume method and solved numerically by SIMPLE algorithm. The computations were carried out for a wide range of the Rayleigh number ($10^4 \leqslant Ra \leqslant 10^7$), Hartman number ($0 \leqslant Ha \leqslant 100$) and solid volume fraction ($0 \leqslant \phi \leqslant 0.05$). The results show that at $Ra = 10^4$ and 10^5 the enhancement of the Nusselt number due to presence of nanoparticles increases with the Hartman number, but at higher Rayleigh number, a reduction has been observed. In addition it was observed that the entropy generation is decreased when the nanoparticles are present, while the magnetic field generally increases the magnitude of the entropy generation.

1. Introduction

Magnetohydrodynamic (MHD) flow when especially associated with heat transfer has received considerable attention in the recent years because of their wide variety of application in engineering areas, such as crystal growth in liquid, cooling of nuclear reactor, electronic package, microelectronic devices, and solar technology. In the case of free convection of an electrically conducting fluid when the magnetic field is present, there are two body forces, a buoyancy force and a Lorentz force. They interact with each other and influence the flow and heat transfer, so that it is important to study the detailed characteristics of transport phenomena in such a process to have a better product with improved design.

Several studies have been performed in recent years on the effect of the magnetic field on natural convection flow and heat transfer in cavities [1–4]. Kandaswamy et al. [1] studied the magnetoconvection flow in a cavity with partially active vertical walls. They have considered nine different positions of active zone for different value of the Rayleigh *Ra* and Hartman *Ha* numbers. It has been found that the average Nusselt number decreases with an increase of *Ha* and increases with the Rayleigh number. Also, for an enough large magnetic field the convection mode of heat transfer is converted into a conduction mode. Pirmohammadi and Ghassemi [2] considered the effect of the magnetic field on convection heat transfer inside a tilted square enclosure. Their study showed that the heat transfer mechanism and flow characteristics inside the enclosure depend strongly upon both magnetic field and inclination angle. Saleh et al. [3] considered numerically natural convection in a porous trapezoidal enclosure with an inclined magnetic field. The heat transfer and fluid flow for different value of Rayleigh, Hartman and magnetic field inclination angle has been studied. They found, that an optimum reducing of the heat transfer rate was obtained for an acute trapezoidal enclosure and large magnetic field in the horizontal direction. Further, Grosan et al. [4] have studied the effects of the magnetic field and internal heat generation on the free convection in a rectangular cavity filled with a porous medium.

With the growing demand for efficient cooling systems, particularly in the electronics industry, more effective coolants are required to keep the temperature of electronic components below safe limits, so that the heat transfer enhancement in engineering is one of the hottest topics in research. Use of nanofluids is an innovative technique to enhance heat transfer [5]. Nanotechnology has been widely used in industry since materials with sizes of nanometers possess unique physical and chemical properties. Nano-scale particle added fluids are called as nanofluid which is firstly introduced by Cho [5]. Use of metallic nanoparticles with high thermal

* Corresponding author.
E-mail address: popm.ioan@yahoo.co.uk (I. Pop).

0045-7930/$ - see front matter © 2012 Elsevier Ltd. All rights reserved.
http://dx.doi.org/10.1016/j.compfluid.2012.11.014

Nomenclature

c_p	specific heat capacity (J/K)
Ec	Eckert number
g	gravitational acceleration (m/s^2)
Gr	Grashof number, $\beta g H^4 q''/(k\upsilon^2)_f$
H	height of the cavity (m)
Ha	Hartman number, $B_0 H\sqrt{\sigma_f/\mu_f}$
k	thermal conductivity (W/mK)
k_b	Boltzmann's constant, 1.38065×10^{-23}
Nu	Nusselt number
Nu^*	Nusselt ratio, $Nu_m/Nu_m\|_{\phi=0}$
Nu^{**}	Nusselt ratio, $Nu_m/Nu_m\|_{Ha=0}$
p	pressure (N/m^2)
P	dimensionless pressure,
Pr	Prandtl number, υ_f/α_f
Ra	Rayleigh number, $\beta g H^4 q''/(k\upsilon\alpha)_f$
S	entropy generation (W/m^3 K)
S^*	entropy generation ratio, $S/S\|_{\phi=0}$
S^{**}	entropy generation ratio, $S/S\|_{Ha=0}$
S'	dimensionless of entropy generation
T	temperature *(K)*
u, v	components of velocity (m/s)
U, V	dimensionless of velocity component
W	width of the cavity (m)
x, y	dimensional Cartesian coordinates (m)
X, Y	dimensionless Cartesian coordinates
CW	Clockwise
CCW	Counter Clockwise

Greek letters

α	thermal diffusivity, $k/(\rho c_p)$ (m^2/s)
β	coefficient of volume expansion (K^{-1})
ϕ	solid volume fraction
γ	electrical conductivity ratio, σ_s/σ_f
μ	dynamic viscosity (Pa s)
θ	dimensionless temperature
ρ	density (kg/m^3)
σ	electrical conductivity
υ	kinematics viscosity(m^2/s)

Subscripts

f	fluid
m	average
nf	nanofluid
o	reference state
s	solid
w	wall

conductivity will increase the effective thermal conductivity of these types of fluid remarkably. Because nanofluid consists of very small sized solid particles, therefore in low solid concentration it is reasonable to consider nanofluid as a single phase flow [6]. There are many numerical studies on natural convection flow of nanofluid in different geometries. The computational studies are very disputed, because the majority results have reported an enhancement in heat transfer due to the presence of nanoparticles [7–14]. On the other hand, some researchers predicted deterioration in heat transfer [15–17]. It seems that the first numerical study of natural convection of Copper (Cu)–water nanofluid in a two-dimensional enclosure was done by Khanafer et al. [7]. The nanofluid in the enclosure was assumed to be in single phase. It was found that for any given Grashof number, the average Nusselt number increased with the solid volume concentration parameter. Mahmoudi et al. [8] investigated numerically the effect of position of horizontal heat source on the left vertical wall of a cavity filled with Cu–water nanofluid. Their results showed that the presence of nanoparticles at low Ra was more pronounced; also when the heat source was located close to the top horizontal wall, nanofluid was more effective. Oztop and Abu-Nada [9] considered natural convection in partially heated enclosures having different aspect ratio and filled with nanofluid. They found that the heat transfer was more pronounced at low aspect ratio and high volume fraction of nanoparticles. Aminossadati and Ghasemi [10] considered the effect of apex angle, position and dimension of heat source on fluid flow and heat transfer in a triangular enclosure using nanofluid. They found that at low Rayleigh numbers, the heat transfer rate continuously increases with the enclosure apex angle and decreases with the distance of the heat source from the left vertex. Recently, Abu-Nada [15] and Abu-Nada et al. [16] studied the effect of variable fluid properties of nanofluids on natural convection in an enclosure. They found that the heat transfer is sensitive to thermophysical properties of the nanofluid (specifically viscosity). It has been also found that for $Ra > 10^3$ the average Nusselt number is reduced by increasing the volume fraction of nanoparticles. However, for $Ra = 10^3$, the average Nusselt number is enhanced by increasing the volume fraction of nanoparticles.

Natural convection in trapezoidal enclosures has been the subject of interest for many studies due to its important application in various fields such as electronic components and solar collectors. Although, there are some valuable studies on natural convection in trapezoidal enclosures using pure fluid [18–20], only a few works considered the effect of nanofluid [21,22]. But no attempt was made to optimize the problem. This can be done by using the Entropy Generation Minimization technique as introduced by Bejan [23]. However, there are only a few studies that consider the second thermodynamic laws in the presence of nanofluids [24–28]. Shahi et al. [24] numerically studied the entropy generation and natural convection in a square cavity with a vertical heat source which is filled with copper–water nanofluid. They have considered entropy generation and heat transfer for a wide range of the Rayleigh number, solid volume fraction parameter and different positions of the heat source. It has been found that the entropy generation decreases with the solid volume fraction. Mahmoudi et al. [25] investigated numerically the effect of the position of heat source in a partially open cavity using nanofluid. The results showed that by moving the open boundary to the top portion of the left vertical wall of the cavity, although the average Nusselt number increases and the total entropy generation decreases, the presence of nanoparticles is less effective in enhancement of the Nusselt number and in the reduction of the entropy generation.

Magnetic nanofluid is a magnetic colloidal suspension of carried liquid and magnetic nanoparticles. The advantage of magnetic nanofluid is that fluid flow and heat transfer can be controlled by external magnetic field, which makes it applicable in various fields such as electronic packing, thermal engineering and aerospace. On contrary to extensive studies on heat and mass transfer of nanofluid, there are only a few studies that have considered the effect of magnetic field on nanofluid flows [29–33]. Hamad [29] analytically investigated the natural convection of a nanofluid over a linearly stretching sheet in the presence of a vertical magnetic field. He showed that for a given value of the solid concentration, the heat transfer rate decreases as magnetic field increases. The point in his work is that the effective value of the electric conductivity for nanofluid was not calculated and that in the governing equa-

tions the electric conductivity is set according to the properties of the base fluid. Thus the increase of the solid volume fraction, in a given magnetic field, does not affect the Lorenz force. Ghasemi et al. [30] studied numerically the magnetic field effect on natural convection in a square enclosure filled by a nanofluid. They have used basic mixture model for calculation of effective electric conductivity of nanofluids. Their results showed that the effect of the solid volume fraction on the heat transfer rate strongly depends on the values of the Rayleigh and Hartman numbers. Nemati et al. [31] also considered the effect of the magnetic field on natural convection of nanofluid by using Lattice Boltzmann model. Their results indicated that the averaged Nusselt number increased with increase of the solid volume fraction parameter, while in the presence of a high magnetic field, this effect is decreased.

The main originality of the present work is the second law analysis due to natural convection in a trapezoidal enclosure filled by Cu -water nanofluid in the presence of a magnetic field. To the best of authors' knowledge, no such a study which considers this problem has been reported in the literature yet. The numerical analysis has been performed for a wide range of Rayleigh number, solid volume fraction parameter, Hartman number and different position of the heat source on the lower horizontal wall. The effective thermal conductivity of the nanofluid is that of the model proposed by Patel et al. [34]. Also, the viscosity of the nanofluid used is that of Brinkman [35] and the effective electrical conductivity is that proposed by Maxwell [36]. The results are presented in the form of entropy generation, streamlines, isotherms and average and local Nusselt numbers.

2. Problem definition and mathematical formulation

Fig. 1 displays schematically the configuration of the two-dimensional trapezoidal enclosure considered in this study. The left vertical wall and the diagonal wall are kept at a constant low temperature T_0 and the horizontal walls are assumed thermally adiabatic. A heat source with the length $l = 2H/5$ is located on the bottom horizontal wall with its position d that is changes with respect to the left vertical wall. Here H is the height of the cavity. It is assumed that both the fluid phase and nanoparticles are in thermal equilibrium and there is no slip between them. Except for the density the properties of the nanoparticles and the base fluid (water) are taken to be constant. Table 1 presents thermo physical properties of water and copper at the reference temperature. It is further assumed that the Boussinesq approximation is valid for buoyancy force. Under these assumptions, the conservation equation of mass, momentum, energy and entropy generation in a two dimensional Cartesian coordinate system are

$$\frac{\partial u}{\partial x}+\frac{\partial v}{\partial y}=0 \tag{1}$$

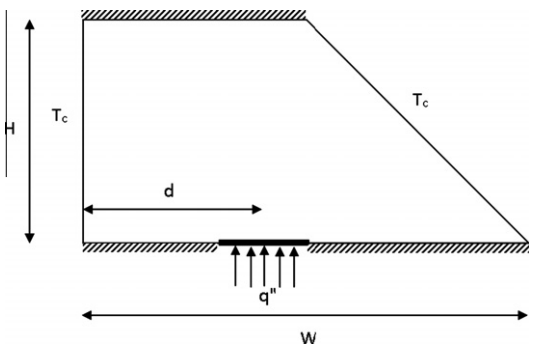

Fig. 1. Schematic configuration of the studied problems.

Table 1
Thermophysical properties of water and copper.

Property	Water	Copper
c_p	4179	383
ρ	997.1	8954
k	0.6	400
β	2.1×10^{-4}	1.67×10^{-5}
σ	0.05	5.96×10^{7}

$$u\frac{\partial u}{\partial x}+v\frac{\partial u}{\partial y}=-\frac{1}{\rho_{nf}}\frac{\partial p}{\partial x}+\upsilon_{nf}\left(\frac{\partial^2 u}{\partial x^2}+\frac{\partial^2 u}{\partial y^2}\right)-\frac{\sigma_{nf}B_0^2}{\rho_{nf}}u \tag{2}$$

$$u\frac{\partial v}{\partial x}+v\frac{\partial v}{\partial y}=-\frac{1}{\rho_{nf}}\frac{\partial p}{\partial y}+\upsilon_{nf}\left(\frac{\partial^2 v}{\partial x^2}+\frac{\partial^2 v}{\partial y^2}\right)+\frac{g}{\rho_{nf}}(T-T_\infty)\times[\phi\rho_{s,0}\beta_s+(1-\phi)\rho_{f,0}\beta_f] \tag{3}$$

$$u\frac{\partial T}{\partial x}+v\frac{\partial T}{\partial y}=\alpha_{nf}\left(\frac{\partial^2 T}{\partial x^2}+\frac{\partial^2 T}{\partial y^2}\right) \tag{4}$$

$$S=\frac{k_{nf}}{T^2}\left[\left(\frac{\partial T}{\partial x}\right)^2+\left(\frac{\partial T}{\partial y}\right)^2\right]+\frac{\mu_{nf}}{T}\left[2\left\{\left(\frac{\partial u}{\partial x}\right)^2+\left(\frac{\partial v}{\partial y}\right)^2\right\}+\left(\frac{\partial u}{\partial y}+\frac{\partial v}{\partial x}\right)^2\right]+\frac{\sigma_{nf}B_0^2}{T}u^2 \quad [44] \tag{5}$$

where $\alpha_{nf}=k_{nf}/(\rho c_p)_{nf}$ is the effective thermal diffusivity of the nanofluid. Further, the effective density of nanofluid at the reference temperature can be defined as

$$\rho_{nf,0}=(1-\phi)\rho_{f,o}+\phi\rho_{s,o} \tag{6}$$

Here $\rho_{nf,0}$, $\rho_{f,0}$, $\rho_{s,0}$ and ϕ are the density of nanofluid, density of base fluid, density of nanoparticles and volume fraction of the nanoparticles, respectively.

The heat capacitance of the nanofluid can be given as

$$(\rho c_p)_{nf}=(1-\phi)(\rho c_p)_f+\phi(\rho c_p)_s \tag{7}$$

The effective thermal conductivity of nanofluid is calculated using the Patel et al. [34] model as follows

$$\frac{k_{eff}}{k_f}=1+\frac{k_pA_p}{k_fA_f}+ck_pPe\frac{A_p}{k_fA_f} \tag{8}$$

where c is a constant and must be determined experimentally (for the current study $c = 3.6\times10^4$), A_p/A_f and Pe are defined as

$$\frac{A_p}{A_f}=\frac{d_f}{d_p}\frac{\phi}{(1-\phi)},Pe=\frac{u_pd_p}{\alpha_f} \tag{9}$$

with d_p being the diameter of the solid particles that in this study is assumed to be equal to 100 nm, d_f is the molecular size of liquid that is taken as 2 Å for water. Also u_p is the Brownian motion velocity of nanoparticles which is defined as

$$u_p=\frac{2k_bT}{\pi\mu_fd_p^2} \tag{10}$$

where k_b is the Boltzmann constant. Further, the effective viscosity of nanofluid is calculated using the Brinkman model [35],

$$\mu_{nf}=\frac{\mu_f}{(1-\phi)^{2.5}} \tag{11}$$

and the effective electrical conductivity of nanofluid was presented by Maxwell [36] as

$$\frac{\sigma_{nf}}{\sigma_f}=1+\frac{3(\gamma-1)\phi}{(\gamma+2)-(\gamma-1)\phi} \tag{12}$$

where $\gamma = \sigma_s/\sigma_f$.

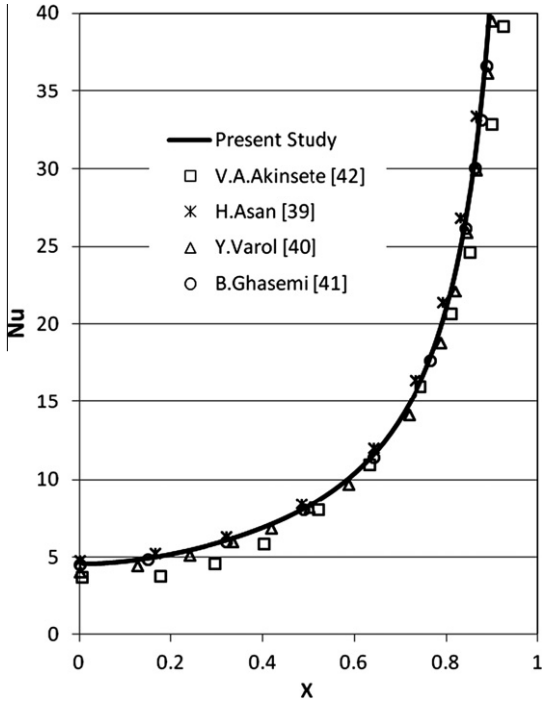

Fig. 2. Comparison of local Nusselt numbers for triangular enclosure with references in order to validate inclined wall boundary condition.

Table 2
Result of grid independence examination.

Number of grids in X–Y	Nu_m
61 × 31	7.403
81 × 41	7.283
101 × 51	7.215
121 × 61	7.167
141 × 71	7.138
161 × 81	7.116
181 × 91	7.098
201 × 101	7.083

Table 3
Comparison of results obtained in this study by [42].

	Nu_m		
	Present	De Vahl Davis[42]	Error (%)
$Ra = 10^4$	2.248	2.242	0.267
$Ra = 10^5$	4.503	4.523	0.444
$Ra = 10^6$	9.147	9.035	1.24

Table 4
Comparison of average Nusselt number with previous works for different Gr number.

	Ha	Present study	Venkatachalappa and Subbaraya [43]	Error (%)
$Gr = 10^4$	0	2.5294	2.5188	0.42
	10	2.2375	2.2234	0.63
	50	1.0884	1.0856	0.26
	100	1.0132	1.0132	0.22
$Gr = 10^5$	0	5.0787	4.9198	3.23
	10	4.9681	4.8053	3.39
	50	2.9894	2.8442	5.1
	100	1.4785	1.4317	3.27

Eqs. (1)–(4) can be converted to the dimensionless form by defining the following variables

$$X = \frac{x}{H}, Y = \frac{y}{H}, U = \frac{uH}{\alpha_f}, V = \frac{vH}{\alpha_f}, \theta = \frac{(T - T_C)k_f}{q''H}, P = \frac{p}{\rho_{nf}}\frac{H^2}{\alpha_f^2} \quad (13)$$

Thus, using these variables leads to the following dimensionless forms of the governing Eqs. (1)–(4)

$$\frac{\partial U}{\partial X} + \frac{\partial V}{\partial Y} = 0 \quad (14)$$

$$U\frac{\partial U}{\partial X} + V\frac{\partial U}{\partial Y} = -\frac{\partial P}{\partial X} + \frac{\mu_{nf}}{\rho_{nf}\alpha_f}\left(\frac{\partial^2 U}{\partial X^2} + \frac{\partial^2 U}{\partial Y^2}\right) - Ha^2 \cdot Pr \cdot \frac{\sigma_{nf}}{\sigma_f}\cdot\frac{\rho_f}{\rho_{nf}}U \quad (15)$$

$$U\frac{\partial V}{\partial X} + V\frac{\partial V}{\partial Y} = -\frac{\partial P}{\partial Y} + \frac{\mu_{nf}}{\rho_{nf}\alpha_f}\left(\frac{\partial^2 V}{\partial X^2} + \frac{\partial^2 V}{\partial Y^2}\right) + Ra \cdot Pr \cdot \frac{\rho_{f,0}}{\rho_{nf,0}}\left(1 - \phi + \phi\frac{\rho_s\beta_s}{\rho_f\beta_f}\right)\theta \quad (16)$$

$$U\frac{\partial \theta}{\partial X} + V\frac{\partial \theta}{\partial Y} = \frac{\alpha_{nf}}{\alpha_f}\left(\frac{\partial^2 \theta}{\partial X^2} + \frac{\partial^2 \theta}{\partial Y^2}\right) \quad (17)$$

And also the dimensionless form of the local entropy generation can be expressed as

$$S'' = \frac{k_{nf}}{k_f}\cdot\frac{1}{(\theta + T^*)^2}\left[\left(\frac{\partial\theta}{\partial X}\right)^2 + \left(\frac{\partial\theta}{\partial Y}\right)^2\right] + \frac{1}{\theta + T^*}\cdot\frac{\mu_{nf}}{\mu_f}\cdot Ec \cdot Pr \cdot \left[2\left\{\left(\frac{\partial U}{\partial X}\right)^2 + \left(\frac{\partial V}{\partial Y}\right)^2\right\} + \left(\frac{\partial U}{\partial Y} + \frac{\partial V}{\partial X}\right)^2\right] + \frac{1}{\theta + T^*}\cdot\frac{\sigma_{nf}}{\sigma_f}\cdot Ec \cdot Pr \cdot Ha^2 \cdot U^2 \quad (18)$$

where T^*, S' and Ec are defined as

$$T^* = \frac{Tck_f}{q''H}, \quad S' = S\frac{H^2}{k_f}, \quad Ec = \frac{\alpha_f^2 k_f}{H^3(C_p)_f q''} \quad (19)$$

The boundary conditions are in the following forms:

$u = v = 0$ at $x = 0$ $0 \leqslant y \leqslant$ H,
$u = v = 0$ at $y = 0$ $0 \leqslant x \leqslant$ W
$u = v = 0$ at $y = H$ $0 \leqslant x \leqslant$ W/2
$u = v = 0$ at diagonal wall

$T = T_C$ at diagonal wall
$T = T_C$ at $x = 0$ $0 \leqslant y \leqslant$ H
$\frac{\partial T}{\partial y} = 0$ at $y = 0$ $0 \leqslant$ $x \leqslant (d - l/2)$and$(d + l/2) \leqslant$ $x \leqslant W$
$\frac{\partial T}{\partial y} = 0$ at $y =$ H $0 \leqslant x \leqslant W/2$

At the heat source's surface: $\frac{\partial T}{\partial y} = -q''/k_{nf}$

In order to estimate the heat transfer enhancement, we have calculated the local (Nu) and average (Nu_m) Nusselt numbers for the heat source wall as follows

$$Nu = \frac{1}{\theta|_{\text{heat source wall}}} \quad (20)$$

$$Nu_m = \frac{\int_{\text{heat source}} Nudn}{\int_{\text{heat source}} dn} \quad (21)$$

In order to present the effect of nanoparticles and magnetic field on the average Nusselt number and total entropy generation, the following Nusselt ration and total entropy generation ration are defined.

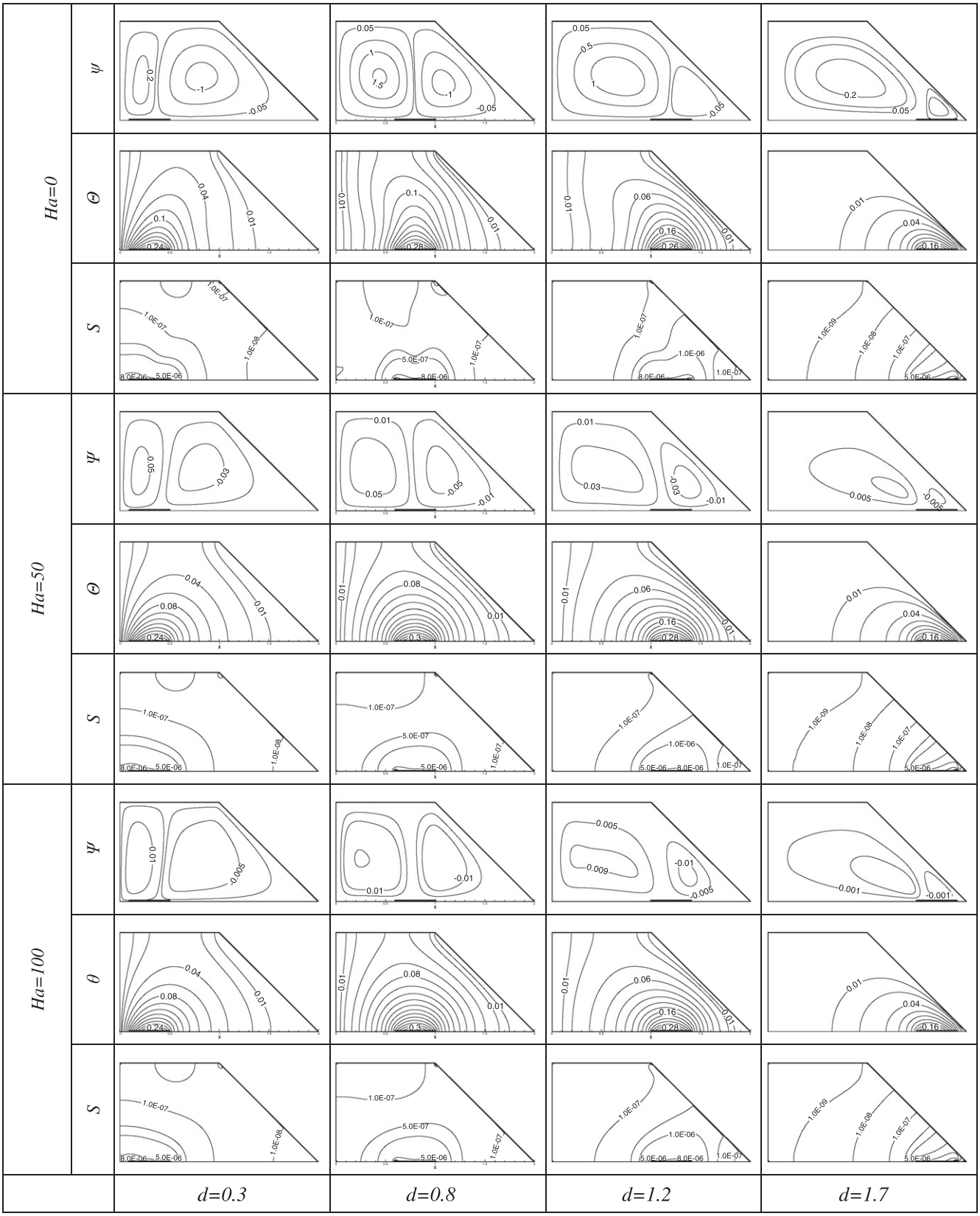

Fig. 3. Streamlines, Isothermal lines and local entropy generation at $Ra = 10^4$ for different Hartman numbers and position of heat source using $\phi = 0$.

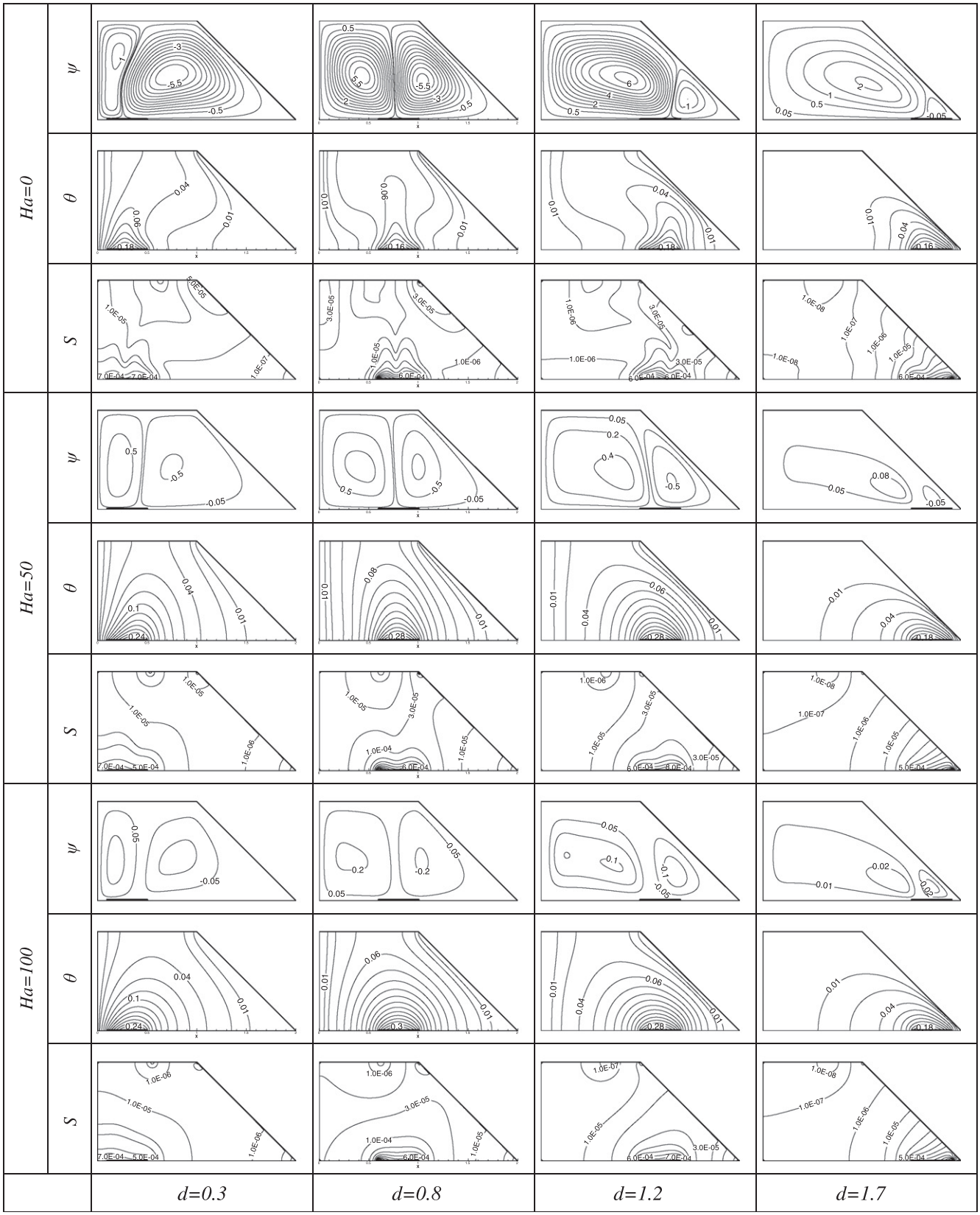

Fig. 4. Streamlines, Isothermal lines and local entropy generation at $Ra = 10^5$ for different Hartman numbers and position of heat source using $\phi = 0$.

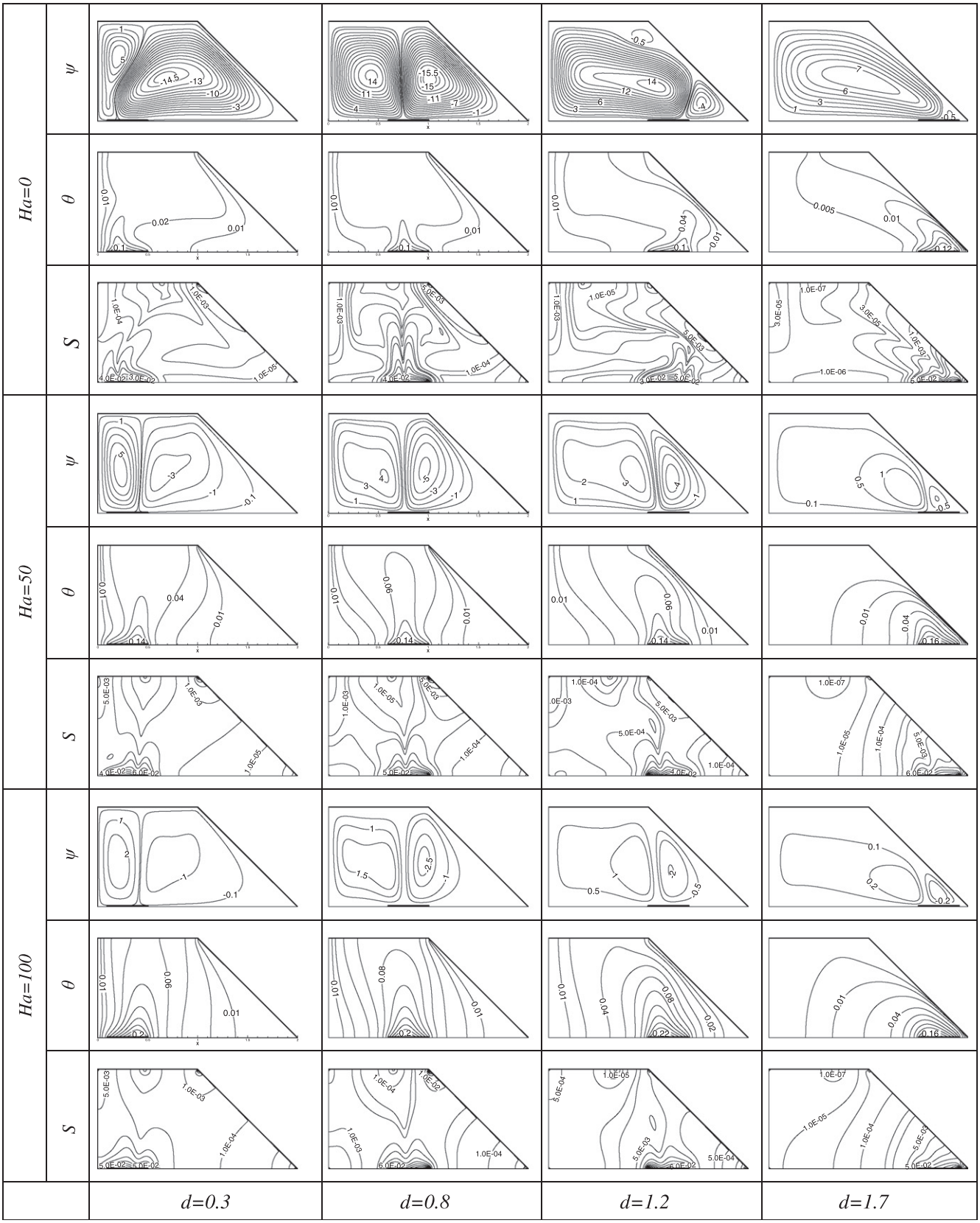

Fig. 5. Streamlines, Isothermal lines and local entropy generation at $Ra = 10^6$ for different Hartman numbers and position of heat source using pure fluid.

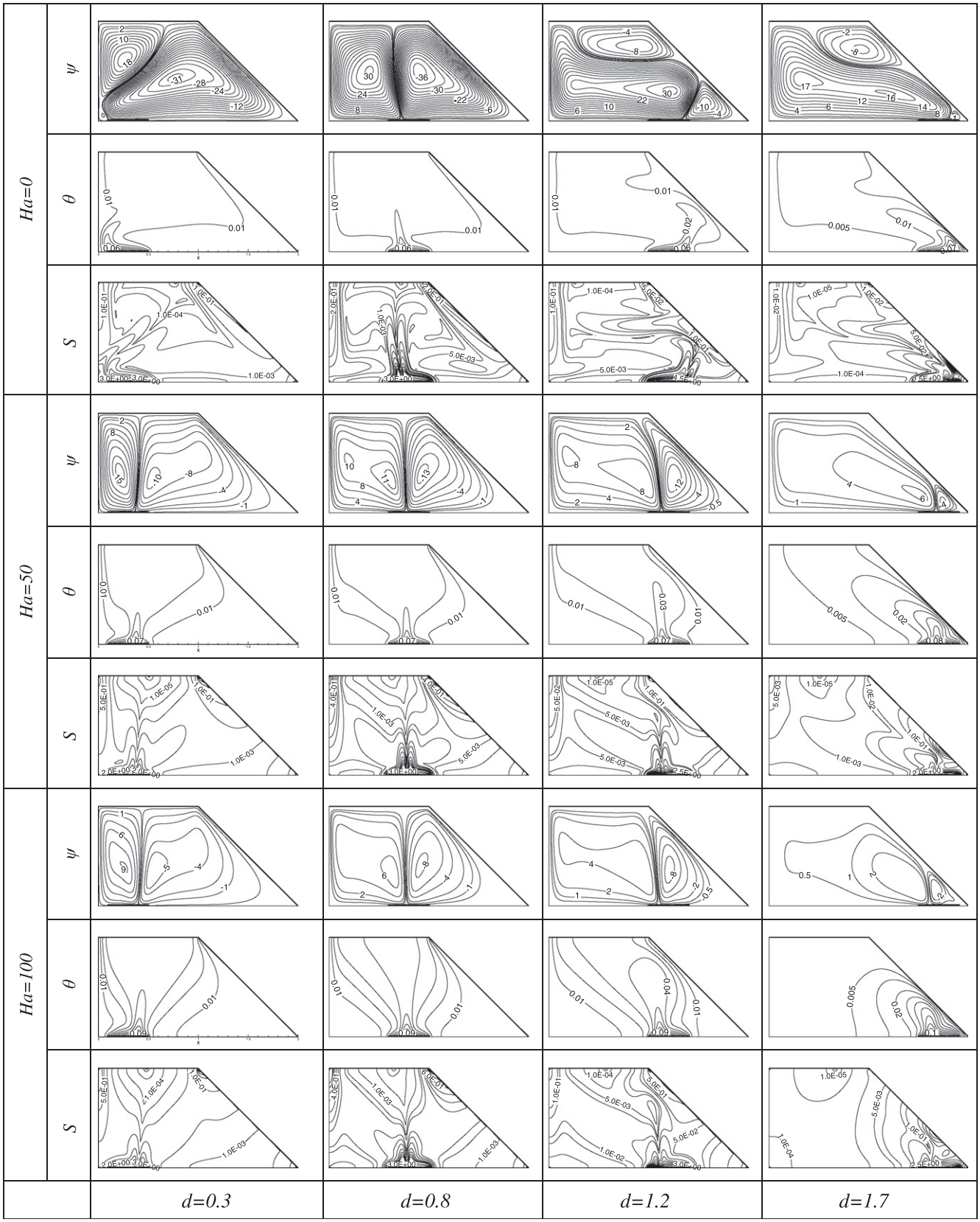

Fig. 6. Streamlines, Isothermal lines and local entropy generation at $Ra = 10^7$ for different Hartman numbers and position of heat source using pure fluid.

$$Nu^{*} = \frac{Nu_m}{Nu_m|_{\phi=0}} \quad \text{and} \quad S^{*} = \frac{S}{S|_{\phi=0}} \tag{22}$$

$$Nu^{**} = \frac{Nu_m}{Nu_m|_{Ha=0}} \quad \text{and} \quad S^{**} = \frac{S}{S|_{Ha=0}} \tag{23}$$

3. Numerical method and validation

A FORTRAN computer code was developed to solve the dimensionless Eqs. (14)–(17) based on the finite volume method using a collocated grid system. A central difference scheme is used to discretize the diffusion terms, whereas upwind differences are adopted for the convection terms. The resulting discretized equations have been solved iteratively through strongly implicit procedure (SIP) (Ferziger and Peric [37]). The SIMPLE algorithm ([38]) has been adopted for the pressure velocity coupling. In this study, a regular rectangular domain is used. The inclined wall of the enclosure is approximated with stair case-like zigzag lines and the grid cells outside of the triangular domain are assumed inactive. This method has been used before by Asan and Namli [39], Varol et al. [40], and Ghasemi and Aminossadati [10,41]. The local Nusselt number Nu on the inclined wall of a triangular enclosure at AR = 0.25 and Ra = 2772 shows a good agreement with the references in Fig. 2. To allow grid-independent examination, the numerical procedure has been conducted for different grid resolutions. Table 2 demonstrates the influence of number of grid points for a test case of fluid confined within the present configuration. The results show that the grid system of 181×91 is good enough to obtain accurate results. The results have been validated for the natural convection flow in an enclosed cavity filled by a regular fluid ($\phi = 0$) and $Ha = 0$ (magnetic field is absent), as reported by De Vahl Davis [42]. Results are given in Table 3 and it is observed a good agreement. Another test for validation of the current code was performed for the case of natural convection in a rectangular enclosure in the presence of magnetic field. In this test case, the average Nusselt number using different values of the Grashof (Gr) and Hartman (Ha) numbers have been compared with those obtained by Venkatachalappa and Subbaraya [43] and a good agreement with the results was registered (see Table 4).

4. Results and discussion

Figs. 3–6 present the stream lines, isothermal lines and local entropy generation for Ra in the range $Ra = 10^4 - 10^7$, $Ha = 0, 50, 100$ and $\phi = 0$ (regular fluid) at four different values of d. It should be notice that Prandtl number in this study is constant and equal to 6.5. Generally the fluid near the heat source rises up and flows down along the cold right and left walls, and forms two contrary cells in the cavity. As the heat source moves towards the right wall, the left CCW cell grows in size and the right CW cell shrinks. At $Ra = 10^4$, the flow field is weak and the conduction mode of heat transfer in more pronounced. Thus, the maximum temperature of the heat source surface at $d = 0.3$ and, especially, at $d = 1.7$ is lower due to strong conduction and the shorter distance between the heat source and the cold wall. Usually, the presence of the magnetic field suppresses the flow field owing to the retarding effect of Lorenz force. Thus, it is expected that the heat transfer decreases

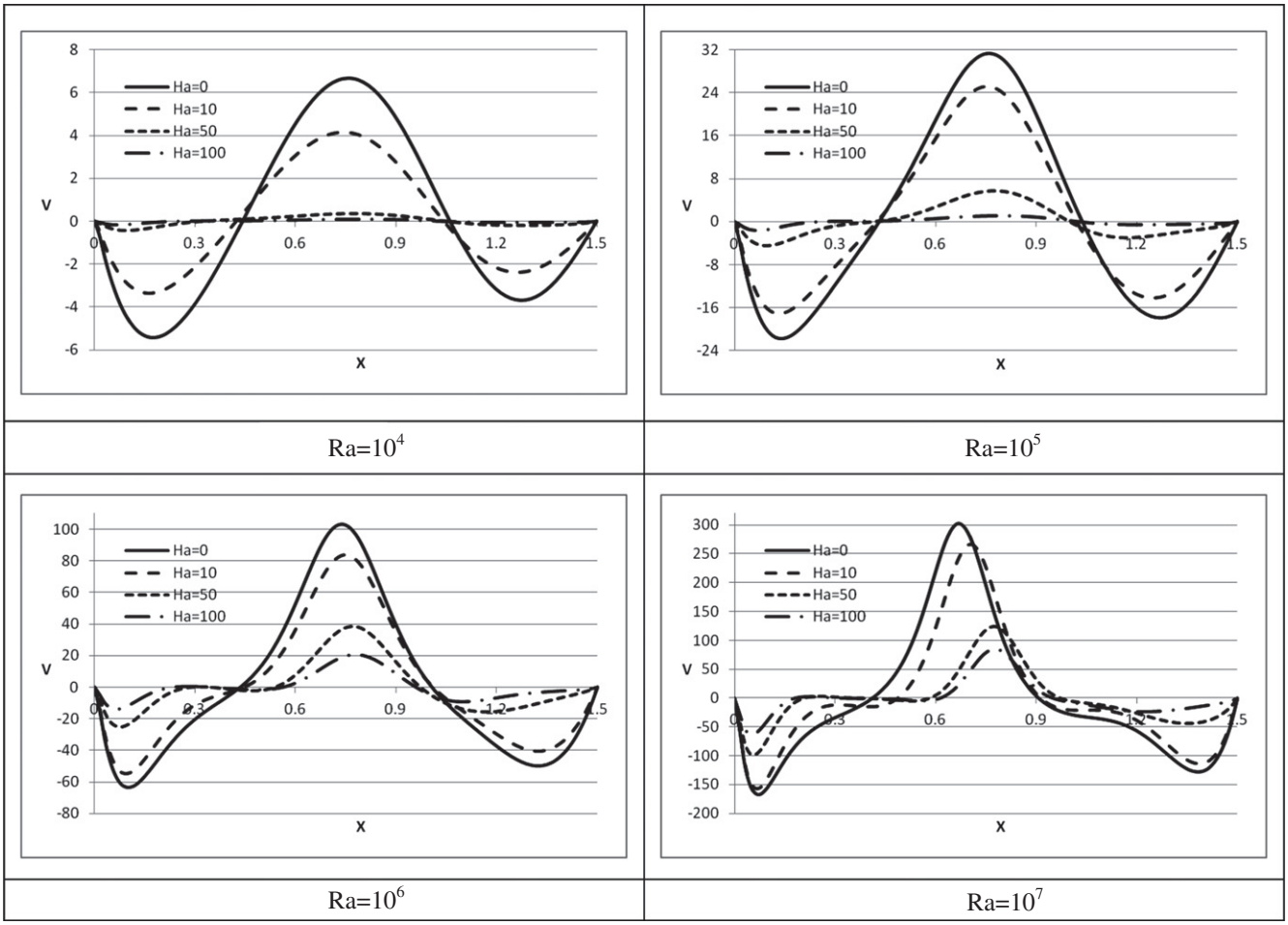

Fig. 7. Variation of vertical velocity component at Y = 0.5 with Hartman number for $d = 0.8$ using $\phi = 0$.

at $d = 1.7$ and the flow field is rather weak, so that even when the magnetic field is absent ($Ha = 0$) isotherms are parallel to each other, indicating that the conduction is dominant. Therefore, the presence of the magnetic field will not influence the heat transfer and temperature of the surface of heat source. Entropy generation in the cavity is due to the two factors, heat transfer irreversibility and fluid friction irreversibility. As can easily be seen in Fig 3 the local entropy is concentrated along the heated surface of the cavity, where the temperature gradient is rather severe. The results for $Ra = 10^5$ and $d = 0.8$ (heat source located almost at the middle of the cavity) illustrated in Fig 4, show that there is enough space to accelerate the flow inside the cavity. Therefore, two rather strong recirculation cells cover the area of enclosure. This is the reason that convection is stronger in this case so that the temperature of heat source surface is equal when $d = 1.7$, where the heat source has shortest distance from the low temperature wall. It is interesting to note that as Ha (Hartman number) increases, the enhancement of heat source surface temperature is registered more at $d = 0.8$ and less at $d = 1.7$, respectively. This is due to the fact that at $d = 0.8$, conduction is weaker compared to other cases. This is also as a result that the heat source is away from the two cold walls and the most part of the heat transfer is done by convection. So at high values of Ha the convection is suppressed, the amount of heat transfer is reduced intensively at $d = 0.8$, but at $d = 1.7$ the temperature of the heat source increases less due to the strong fluid conduction. Therefore for $Ha = 100$, the temperature of the heat source surface at $d = 0.8$ is approximately 87% higher than when $Ha = 0$, but at $d = 1.7$ it is only 12.5%. As can be seen in Fig. 5, at $Ra = 10^6$ (with the increase of the flow intensity) the convection is more pronounced. Thus, since the flow field at $d = 1.7$ is less intensive than other cases, the maximum temperature of heat source is higher. At $Ha = 100$ one can observe an interesting thing, namely that although the parallel isothermal lines at $d = 1.7$ indicates a dominant conduction, while for other values of d this is not seen, but the temperature of the heat source is less than in other cases. It is, generally observed that at $Ra = 10^6$ and an increase of Ha, the small cells grow in size and push the larger cells away. For example, the two small triangular cells at $d = 1.2$ and $Ha = 0$ are connected to each other with the increase of Ha and produces a bigger cell, which covers the third of the cavity. The local entropy generation distribution shows that with the increase of Ra, it becomes more significant within the enclosure due to the existence of larger temperature gradient and also due to the enhancement of velocity level that causes a stronger fluid friction. With further increase of Ra, there is a small change of the flow pattern, as it is depicted for $Ra = 10^7$ in Fig. 6. In the case of $Ha = 0$ (magnetic field absent) a rather big CW cell appears at the top corner of the cavity and besides the inclined wall and also a smaller inclined down corner wall of the cavity for $d = 1.2$ and 1.7. At $d = 0.3$ CCW cell changes to a triangular shape cell and moves upward. But when the magnetic field is imposed ($Ha \neq 0$) on the enclosure, the CCW triangular cell at $d = 1.7$ disappears, while at $d = 1.2$ the two cells connect to each other and make a bigger unicellular pattern. Thus the cavity is covered with two rectangular and triangular cells. At $Ra = 10^7$ the convection is very strong, so that even at $Ha = 100$ the convection in dominant. This behavior is indicated by the nonlinear isothermal lines. Therefore, like for the low values of Ha, at $Ra = 10^6$ but for high values of Ha, the maximum temperature of the heat source surface at $d = 1.7$, despite it is very close to the cold inclined wall, is higher than for other values of d. Fig. 7 presents the vertical velocity profiles at $Y = 0.5$ for $d = 0.8$. As explained before, the velocity profiles are almost flat at high values of Ha and low values of Ra. But at high values of Ra the velocity profiles have comparable values indicating a smal-

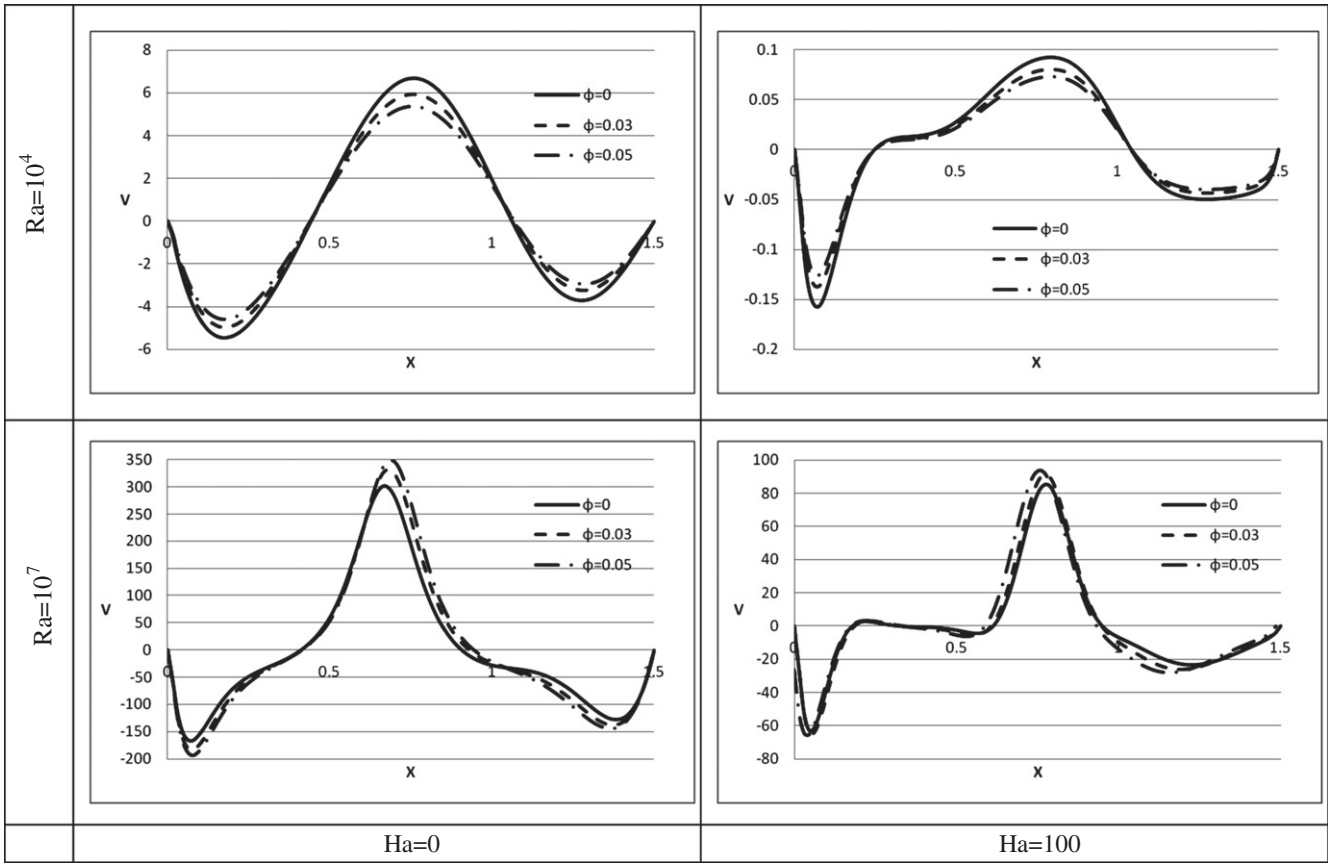

Fig. 8. Variation of vertical velocity component at Y = 0.5 with solid volume fraction at $Ha = 0$, 100 and $Ra = 10^4$, 10^7.

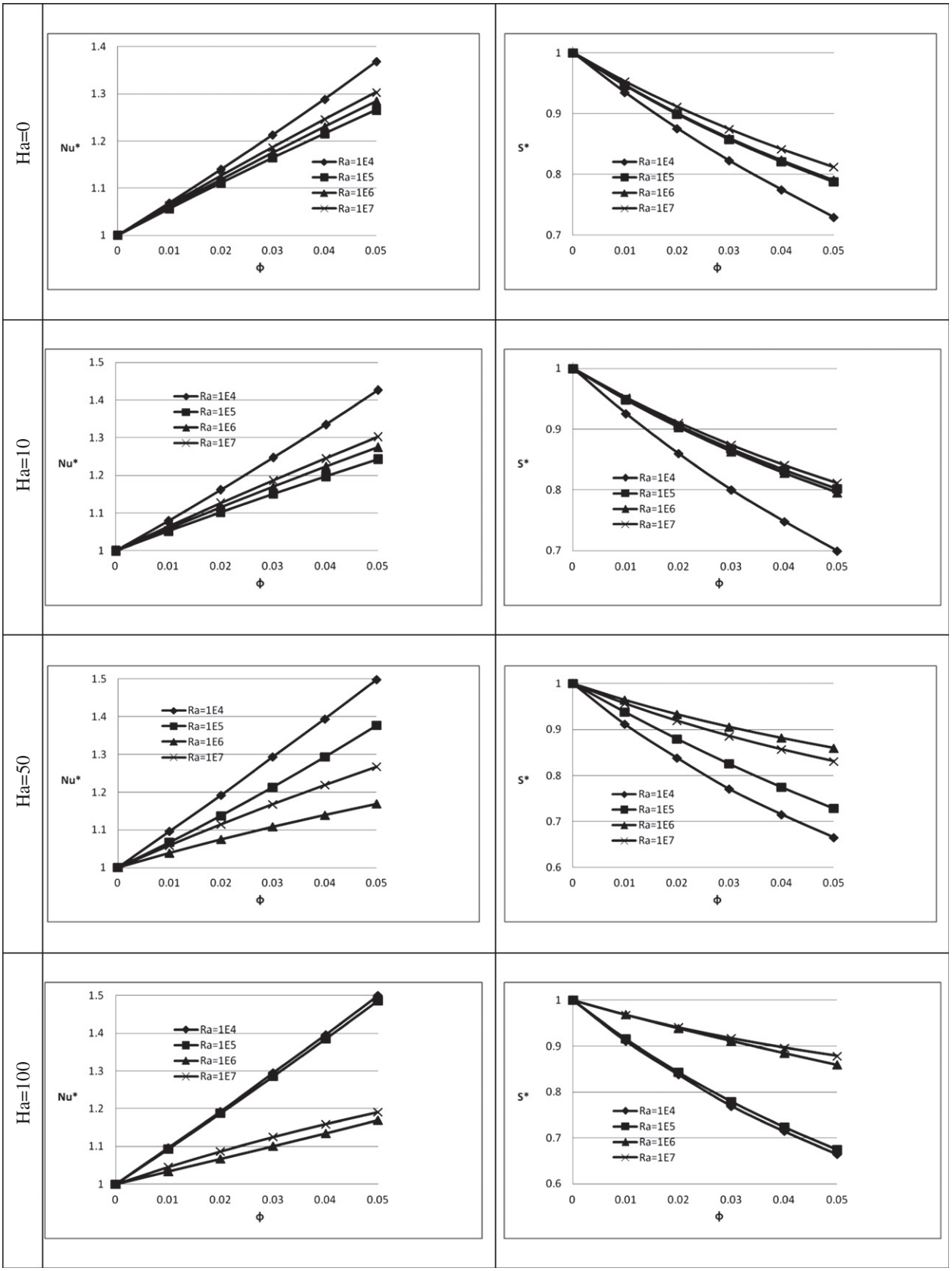

Fig. 9. The effect of solid concentration on the variation of the average Nusselt number and total entropy generation for different values of Rayleigh and Hartman numbers at $d = 0.8$.

ler effect of the magnetic field on the flow field for high values of *Ra*.

Existence of the metallic nanoparticles in the water changes the properties of the base fluid and hence affects the heat transfer and fluid flow characteristics. The presence of high thermal conductive nanoparticles enhances the thermal conductivity of the nanofluids and causes a favorable enhancement of the heat transfer. On the other hand, nanoparticles increase both viscosity and electric conductivity of the nanofluid. The enhancement of nanofluid viscosity increases the fluid friction and hence decreases convection heat transfer. Also, the increase of the electrical conductivity increases the Lorenz force and leads to a substantial suppression of the convection. So the two last effects of nanoparticles are unfavorable from the point of view of heat transfer. The interaction between these parameters controls the heat transfer within the cavity. In order to obtain a better understanding of these three effects, Fig. 8 presents the vertical velocity profiles at $Ra = 10^4 - 10^7$ for $\phi = 0, 0.03, 0.05$ and $Ha = 0$, and 100. At $Ra = 10^4$, since the velocity field is poor, unfavorable increase of viscosity due to presence of nanoparticles is more pronounced than when the buoyancy force increase. Thus, the velocity profiles decrease with the increase of the solid volume nanoparticle parameter ϕ. But at $Ra = 10^7$ the convection is very strong, so that the presence of nanoparticles increases the velocity within the cavity. At $Ha = 100$ the nanoparticle parameter ϕ still increases the vertical velocity field, but due to unfavorable increase of the Lorenz force, the enhancement of velocity with nanoparticles is less than when the magnetic field is absent.

Fig. 9 shows the impact of the nanoparticles on the heat transfer and entropy generation when the magnetic field is present and for different values of *Ra* at $d = 0.8$. As can be seen, the presence of nanoparticles is associated with an increase in the heat transfer and the Nusselt number. It can, therefore, be concluded that regarding the parameters *Ra* and *Ha*, the effect of thermal conductivity enhancement on heat transfer is more consistent than the increase of the viscosity and electric conductivity. The presence of nanoparticles for low Rayleigh numbers, where the heat transfer is dominated by conduction, causes more enhancement in heat transfer. At $Ra = 10^4$, the average Nusselt number Nu_m increases with *Ha* but at $Ha = 50$ the convection is completely suppressed, as can be seen in Fig 3. Thus, an extra magnetic field will not result in an enhancement of the Nusselt numbers Nu or on Nu_m. At $Ra = 10^5$ and $Ha = 100$, the velocity field, as it is observed in Figs. 4 and 7, weakens significantly and conduction is dominated. The nanoparticles have the same effect as that observed for $Ra = 10^4$ on the enhancement of the Nusselt numbers. Although the favorable enhancement of the nanofluid has a dominant effect on the thermal conductivity, it leads to enhancement of the Nusselt numbers, but the unfavorable increase of the electrical conductivity affects on some amount this enhancement. It is clear that at higher values of *Ra* the enhancement of the Nusselt numbers with the solid concentration decrease as *Ha* increases. For example at $Ra = 10^7$ and $Ha = 0$ using 5% solid concentration, the average Nusselt number Nu_m increases by 30% compared to 19% for the case when $Ha = 100$. The presence of nanoparticles has two opposite effects on entropy generation. Enhancement of heat transfer due to the presence of nanoparticles decreases the temperature gradient and leads to a reduction of the entropy generation, but on other side, with the increase of viscosity of nanofluid, the friction losses the increase and leads to an increase of entropy generation. The results show that the temperature gradient is the dominant factor in entropy generation, so with the presence of nanoparticles the entropy generation inside the cavity decreases. The highest reduction of the entropy generation is registered at $Ha = 100$ when $Ra = 10^4$ and 10^5, so that by using 5% solid concentration the entropy generation decreases with 33%.

The results illustrated in Fig. 10 demonstrate the influence of the magnetic field on the average Nusselt number Nu_m and on

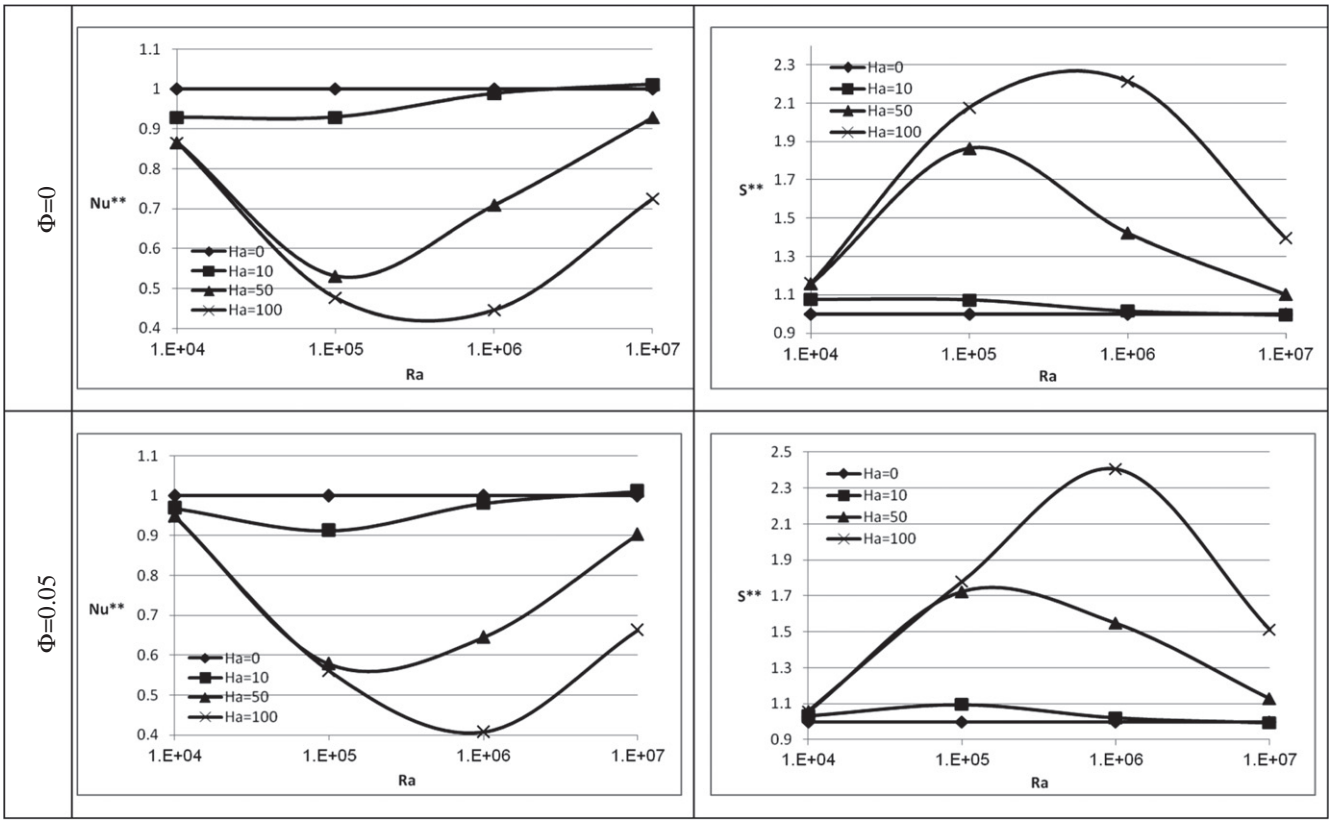

Fig. 10. The effect of Hartman number on the variation of the average Nusselt number and total entropy generation for different values of Rayleigh using $\Phi = 0, 0.05$.

the total entropy generation at $d = 0.8$ for both the pure fluid ($\phi = 0$) and using 5% solid concentration nanoparticles. The results also show that the increase of the magnetic field is mainly associated with the decrease of Nu_m due to the reduction in convection heat transfer. At moderate values of the parameter Ha the highest reduction in Nu_m is registered at $Ra = 10^5$, because even with the increase of Ha to 50, the convection shifts towards the conduction and, therefore, the maximum reduction in heat transfer happens

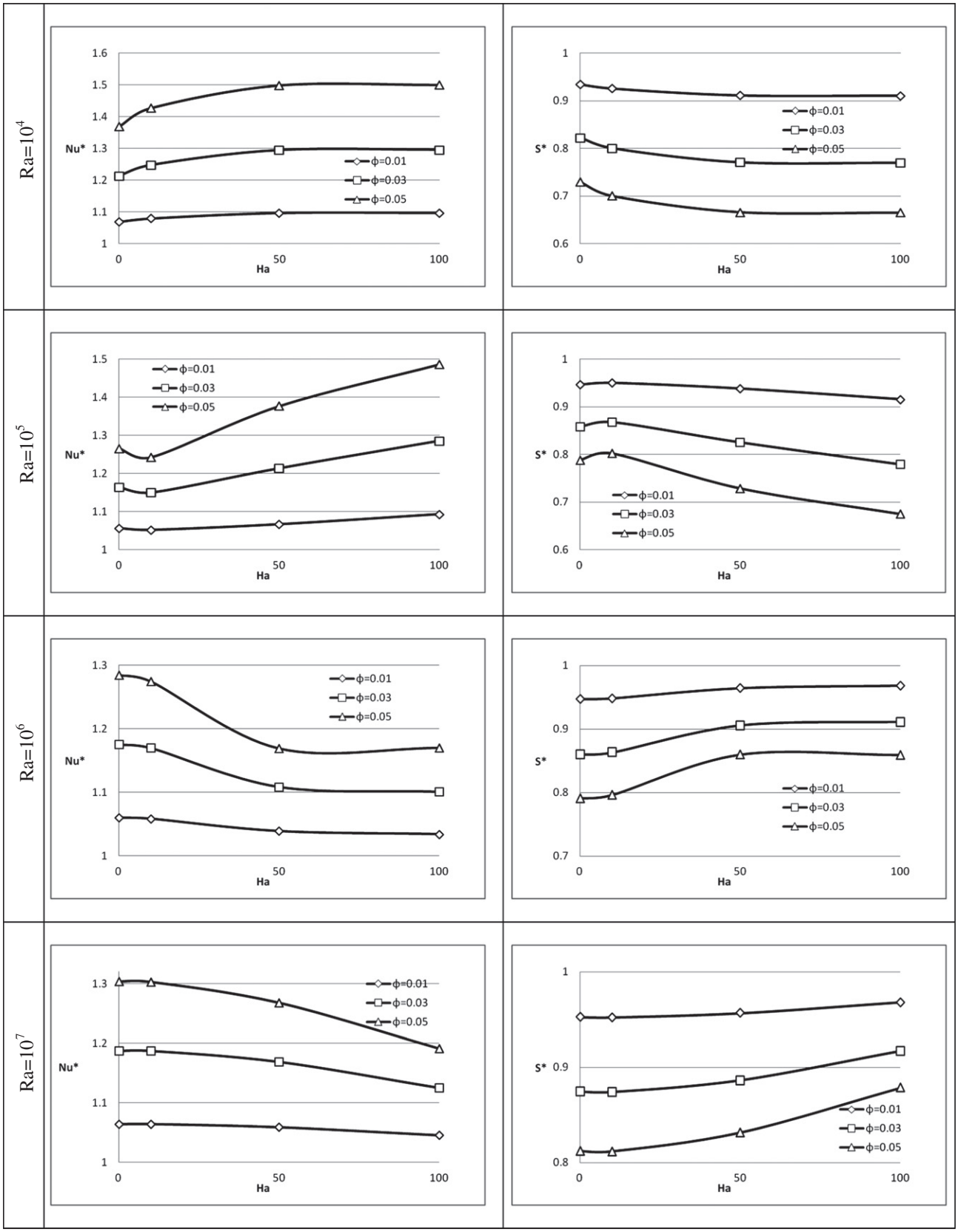

Fig. 11. Variation of Nu^* and S^* versus Hartman number for different value of solid volume fraction and Rayleigh number at $d = 0.8$.

for $Ra = 10^5$. With the further increase of Ha to 100, a further noticeable reduction in the flow field cannot be observed for $Ra = 10^5$, but for $Ra = 10^6$ the velocity field is more suppressed. So as can be seen from Fig. 10, the highest reduction in Nu_m is observed for $Ha = 100$ when $Ra = 10^6$. An increase of the Lorenz forces due to the presence of nanoparticles is an unfavorable effect that leads to reduction of the heat transfer. At $Ra = 10^6$ and 10^7 the convection in the cavity is more pronounced, so that, at $Ra = 10^6$ and $Ha = 100$ the average Nusselt number Nu_m decreases by 55% for pure fluid ($\phi = 0$) compared to 60% in the case of $\phi = 0.05$. At $Ra = 10^4$ as it was presented in Fig. 8, the presence of nanoparticles weakens the velocity field in the cavity. Thus an increase of the magnetic field has less effect on the reduction of convection and average Nusselt number because the flow field was already suppressed by the presence of nanoparticles and hence conduction mode in the cavity is dominant. For a pure fluid ($\phi = 0$) and $Ha = 100$ the average Nusselt number Nu_m decreases by about 14% in respect to $Ha = 0$, but by using 5% solid concentration nanoparticles it decreases only by 5%. With the increase of Ha, although the friction loss is decreased due to reduction of the velocity field, but the heat transfer decreases and the temperature gradient increases, so the total entropy generation increases with Ha. Further as can be seen from Fig. 10, the increase of the magnetic field results in a higher enhancement of the total entropy in the presence of nanoparticles for $Ra > 10^5$ and lower enhancement for low values of Ra. Thus, at $Ra = 10^6$ and $\phi = 0$ the total entropy generation increases by 2.2 times with the increase of Ha from zero to 100 compared to 2.4 times by using 5% solid concentration nanoparticles. A 2.1 times increase of the total entropy is observed for a pure fluid ($\phi = 0$) and 1.8 times for $\phi = 0.05$ when $Ra = 10^5$ Fig. 11 presents the variation of Nu^* and S^* versus Ha using $\phi = 0.01, 0.03, 0.05$. The results show that with the increase of Ha, lower enhancement of Nu^* is observed at $Ra = 10^6$ and 10^7 as a result of the presence of nanoparticles. This is due to the increase of the Lorenz force with metallic nanoparticles. Thus by using 5% solid concentration nanoparticles, the average Nusselt number Nu_m at $Ra = 10^7$ and $Ha = 0$ increases about 30% but at $Ha = 100$, the enhancement reaches to 19%. This behavior for lower value of ϕ is observed with less intensity. For example by using 3% solid concentration nanoparticles, the value of Nu^* decreases from 1.19 to 1.12 with the increase of Ha from zero to 100. On the contrary, at low values of the Rayleigh number, the increase of Ha makes more pronounced the presence of nanoparticles on the enhancement of Nu^*. At $Ra = 10^4$ and 10^5 although the augmentation of the magnetic field increases the total entropy generation, it enhances the reduction of entropy generation as a result of the presence of nanoparticles. For example at $Ra = 10^5$ using 5% solid concentration nanoparticles decreases the total entropy generation by about 21% at $Ha = 0$ but at $Ha = 100$ it decreases by about 32%.

Fig. 12 illustrates the variation of the local Nusselt number Nu along the heat source at $Ra = 10^4, 10^7$ and for $Ha = 0, 100$ at different positions d of the heat source. Generally Nu is higher at the edge of heat source. This is due to the fact that for each value of d, the cold flow at the first contact with the edge of the heat source so, as a result of absorbing heat, a warmer flow pass over the rest surface of heat source and leads to decreases the heat transfer compared to the edges. Since at $Ra = 10^4$, the conduction is dominant, so that the heat transfer and hence Nu is higher at the edge of the heat source in the cases of $d = 0.3$ and 1.7 that is closer to the cold source. Because at $Ra = 10^7$ the convection within the enclosure is stronger, the local Nusselt number increases and also the difference between the edges and middle of the heat source increases. Unlike at $Ra = 10^4$, it is observed that for $d = 0.3$, and $Ra = 10^7$ and $Ha = 0$, the local Nusselt number is higher at the right

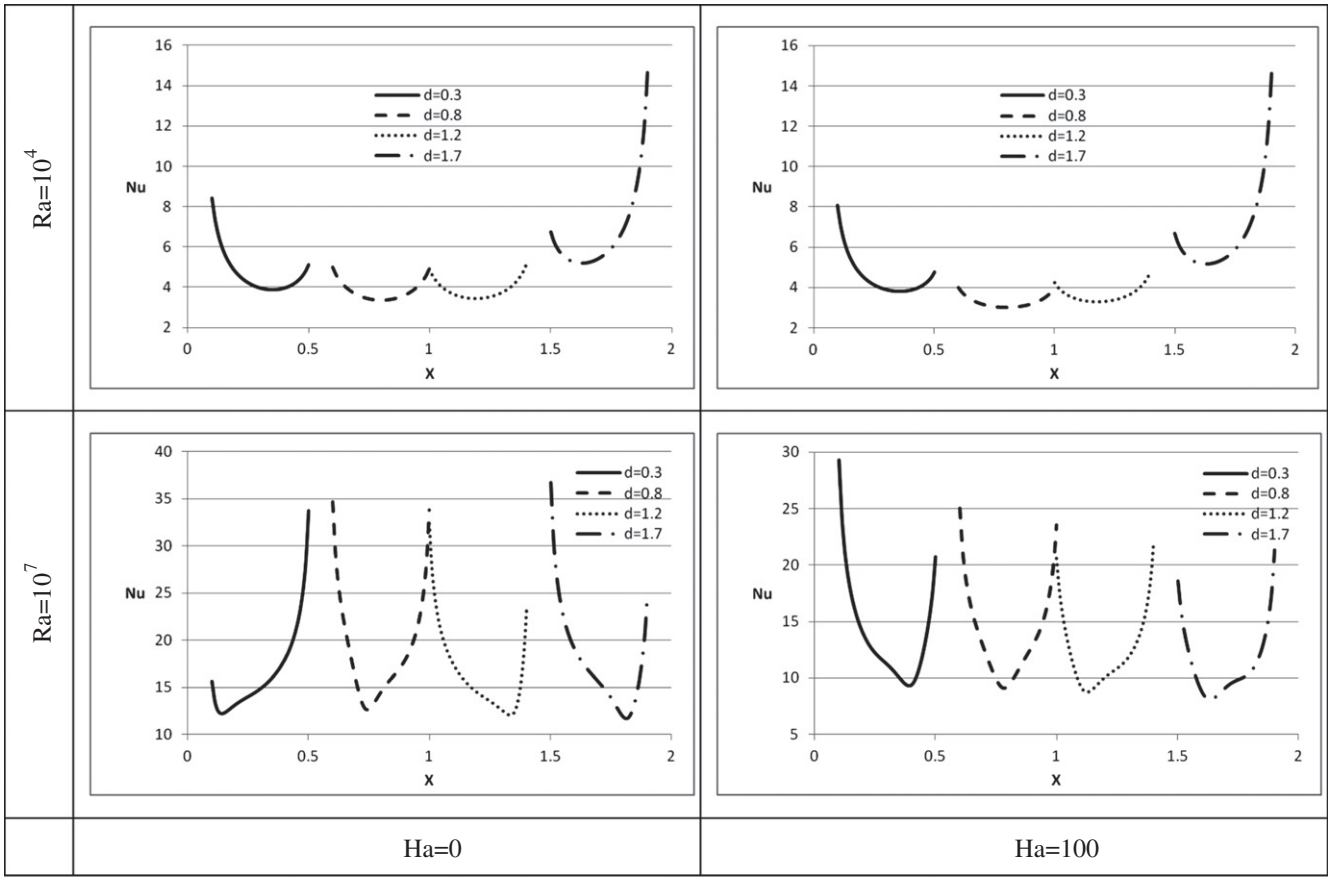

Fig. 12. Local Nusselt number on the heat source surface for different value of Ra, Ha and d using pure fluid.

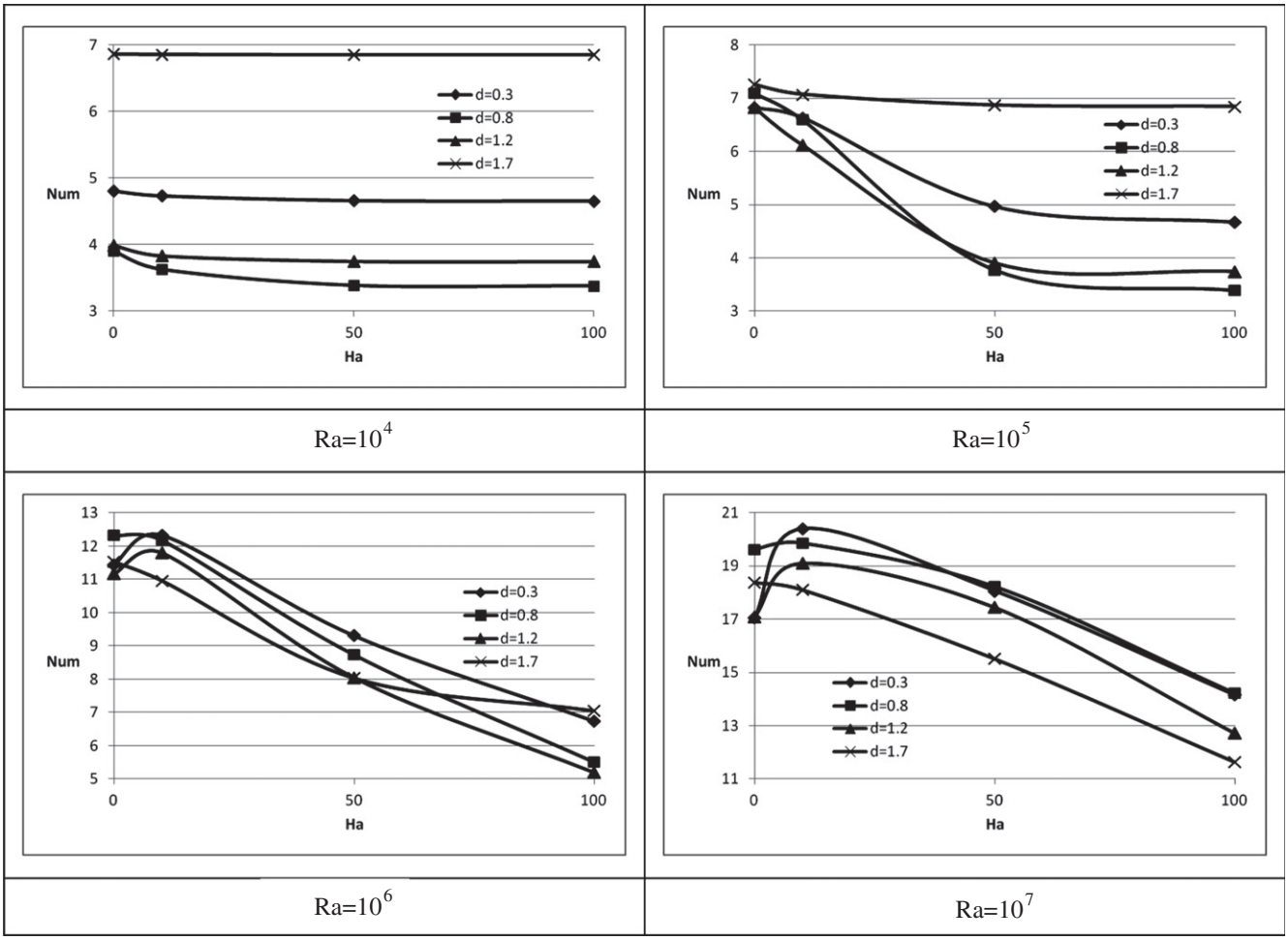

Fig. 13. Variation of average Nusselt number with *Ha* at different position of heat source.

edge of the heat source due to the contact with a strong cold flow, despite the heat source is farther from the cold wall. It can be observed the same behavior at $d = 1.7$ but at the opposite edge. At $Ra = 10^7$ and with the increase of *Ha* the local Nusselt number decreases except in case when $d = 0.3$. At $d = 0.3$ although as a result of the reduction of the convection, the local Nusselt number at the right edge of the heat source decreases intensively, but at the left edge it is observed a considerable enhancement. This is related to the better contact of CCW recirculation cell with the left part of the heat source, as shown in Fig. 6.

Fig. 13 shows the variation of the average Nusselt number Nu_m with the Hartman number *Ha* for different value of *Ra* and d. It is noticed that at $Ra = 10^4$ and 10^5 the highest value of Nu_m is registered for every *Ha* at $d = 1.7$. This is expected since the heat source is closer to cold wall. Since the convection is dominant at $Ra = 10^7$ thus, at $d = 0.3$ and 0.8 (where the flow field is strong), the average Nusselt number is maximum. But at $d = 1.7$ because the convection is not as strong as for other values of *d*, the average Nusselt number is minimum.

Nu^{**} and S^{**} are plotted as a function of *Ra* in Fig. 14 for different values of *Ha* and different positions *d* of the heat source using a pure fluid ($\phi = 0$). It is expected that with augmentation of the magnetic field, the heat transfer and hence the Nusselt number decreases. It is, however, generally true but there are some exceptions. At $d = 0.3$ with the increase of *Ha* to 10, the Nu_m increases at $Ra = 10^6$ and 10^7. This increase is observed even for $Ra = 10^7$ and $Ha = 50$. This could be explained by the fact that with the increase of *Ha* to 10 the CCW recalculating cell that covers the left cold wall of the cavity, gets in contact with the heat source surface (as it is observed in Figs. 5 and 6) and hence the heat transfer increases. This behavior is also observed for $d = 1.2$ and $Ha = 10$. For all value of *d*, except $d = 1.7$ and moderate values of *Ha* the highest reduction in Nu^{**} is occurred at $Ra = 10^5$. This is due to the fact that, at this condition, the heat transfer mechanism is shifted from convection to conduction. Therefore, further increase of the magnetic field will not influence the heat transfer considerably since the conduction is mainly dominant. Thus Nu is approximately kept constant. But at $Ra = 10^6$ the flow field is stronger, and further increase of *Ha* results in more reduction in the convection and Nu_m. On the contrary, at $Ra = 10^7$ because the flow intensity is very high, even at $Ha = 100$, the velocity has a considerable value and hence the magnetic field has less effect on the heat transfer (see Fig. 7). Thus, as it is clearly observed in Fig. 14, the highest reduction of Nu_m at $Ha = 100$ takes place at $Ra = 10^6$. For $d = 1.7$ even at $Ra = 10^5$ and $Ha = 0$ the flow intensity within the enclosure is lower than in the other cases and conduction is mainly dominant (see Fig. 4). Therefore, the increase of *Ha* does not influence considerably the heat transfer. But at $Ra = 10^6$, the flow field being stronger, the presence of the magnetic field is more effective. Generally the presence of the magnetic field is more pronounced at $d = 0.8$ and 1.2 compared to $d = 0.3$ and 1.7. Therefore, the highest and lowest reduction of the heat transfer when $Ra = 10^6$ and $Ha = 100$ are 55% for $d = 0.8$ and 39% for $d = 1.7$, respectively. As already has been explained, with the increase of *Ha* although the friction loss de-

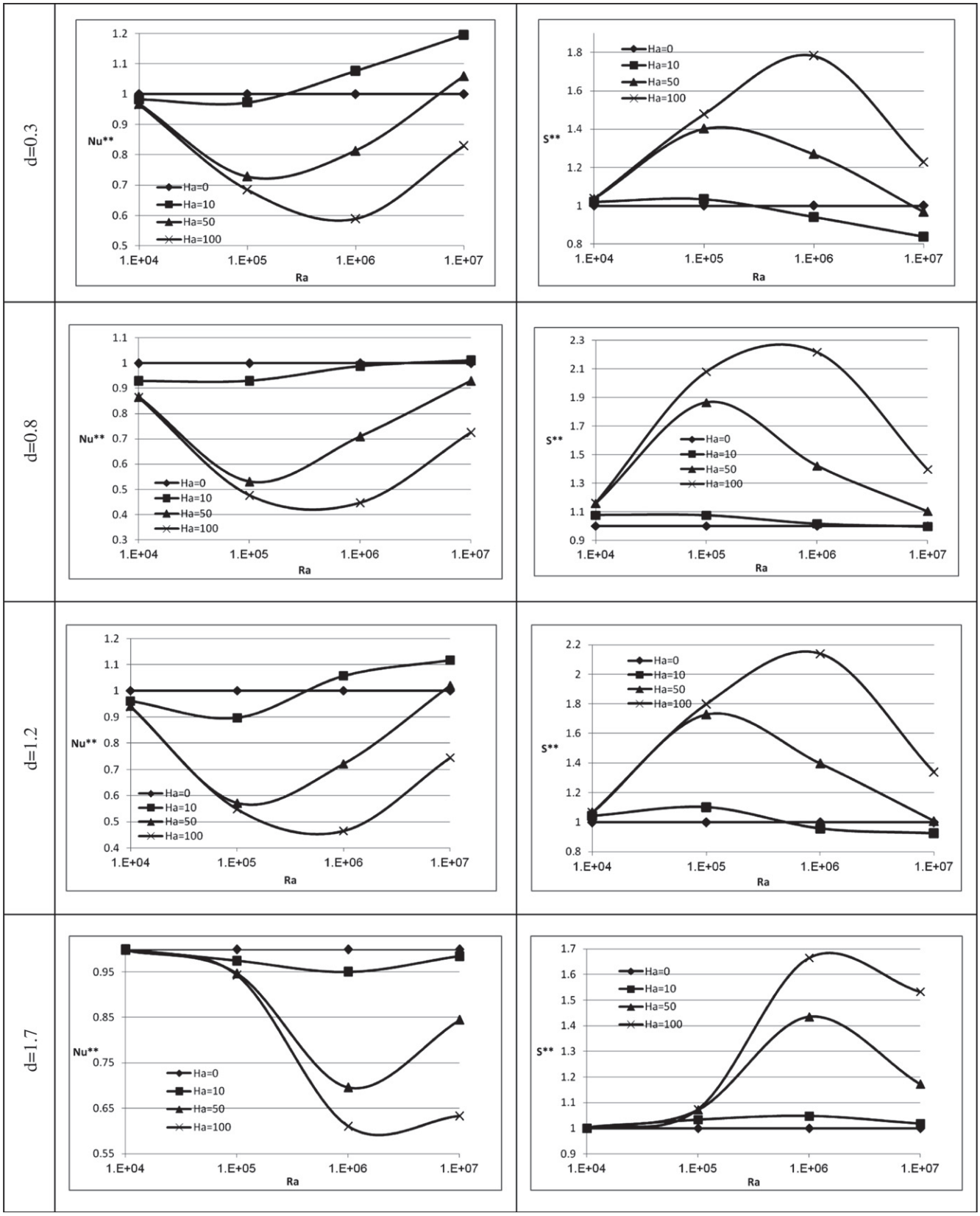

Fig. 14. Variation of Nu^{**} and S^{**} with Ha and Ra at different position of heat source using $\phi = 0$.

creases, due to the reduction of flow intensity, as a result of the reduction of heat transfer, the temperature gradient that is a dominant parameter, the entropy generation increases. Since at high values of Ha, the highest reduction in heat transfer takes place at $Ra = 10^6$, so the highest enhancement of the entropy generation occurs at this value of the Rayleigh number.

5. Conclusion

The numerical code was developed in the present paper to calculate the entropy generation due to the natural convection cooling of a heat source mounted inside a trapezoidal cavity filled by Copper–water nanofluid in the presence of vertical magnetic field. The results were presented for $10^4 \leqslant Ra \leqslant 10^7$, $0 \leqslant Ha \leqslant 100$ and $0 \leqslant \phi \leqslant 0.05$ at different positions d of the heat source on the bottom wall in the form of streamlines, isothermal lines, local and total entropy generation and Nusselt numbers. In view of the obtained results, the following results may be summarized.

It was observed that the entropy generation is decreased with the presence of the nanoparticles, while the magnetic field increases, generally, the entropy generation. The results showed at $Ra = 10^4$ and 10^5, the enhancement of the Nusselt numbers due to the presence of nanoparticles increased with the Hartman number, but at higher values of the Rayleigh number a reduction was registered as a result of higher effect of augmentation of Lorenz force with nanoparticles. Generally, with suppression of the velocity field as a result of inserting magnetic field, the heat transfer and Nusselt numbers decrease but it was observed, in some cases (for example at $d = 0.3, 1.2$ and $Ra = 10^7$), that due to the better contact of the recirculation cells with the heat source, the Nusselt number increases with Ha.

References

[1] Kandaswamy P, Sundari SM, Nithyadevi N. Magnetoconvection in an enclosure with partially active vertical walls. Int J Heat Mass Transfer 2008;51:1946–54.
[2] Pirmohammadi M, Ghassemi M. Effect of magnetic field on convection heat transfer inside a tilted square enclosure. Int Commun Heat Mass Transfer 2009;36:776–80.
[3] Saleh H, Roslan R, Hashim I. Natural convection in a porous trapezoidal enclosure with an inclined magnetic field. Computers Fluids 2011;47:155–64.
[4] Grosan T, Revnic C, Pop I, Ingham DB. Magnetic field and internal heat generation effects on the free convection in a rectangular cavity filled with a porous medium. Int J Heat Mass Transfer 2009;52:1525–33.
[5] Cho SUS. Enhancing thermal conductivity of fluids with nanoparticles. ASME Fluids Eng Division 1995;231:99–105.
[6] Xuan YM, Li Q. Heat transfer enhancement of nanofluid. Int J Heat Fluid Flow 2000;21:58–64.
[7] Khanafer K, Vafai K, Lightstone M. Buoyancy-driven heat transfer enhancement in a two-dimensional enclosure utilizing nanofluids. Int J Heat Mass Transfer 2003;46:3639–53.
[8] Mahmoudi AH, Shahi M, Raouf A, Ghasemian A. Numerical study of natural convection cooling of horizontal heat source mounted in a square cavity filled with nanofluid. Int Commun Heat Mass Transfer 2010;37:1135–41.
[9] Oztop HF, Abu-Nada E. Numerical study of natural convection in partially heated rectangular enclosures filled with nanofluids. Int J Heat Fluid Flow 2008;29:1326–36.
[10] Aminossadati SM, Ghasemi B. Enhanced natural convection in an isosceles triangular enclosure filled with a nanofluid. Comput Math Appl 2011;61:1739–53.
[11] Talebi F, Mahmoudi AH, Shahi M. Numerical study of mixed convection flows in a square lid-driven cavity utilizing nanofluid. Int Commun Heat Mass Transfer 2010;37:79–90.
[12] Mahmoodi M, Hashemi SM. Numerical study of natural convection of a nanofluid in C-shaped enclosures. Int J Thermal Sci 2012;55:76–89.
[13] Sun Q, Pop I. Free convection in a triangle cavity filled with a porous medium saturated with nanofluids with flush mounted heater on the wall. Int J Thermal Sci 2011;50:2141–53.
[14] Farooji VE, Bajestan EE, Niazmand H, Wongwises S. Unconfined laminar nanofluid flow and heat transfer around a square cylinder. Int J Heat Mass Transfer 2012;55:1475–85.
[15] Abu-Nada E. Rayleigh-Bénard convection in nanofluids: Effect of temperature dependent properties. Int J Thermal Sci 2011;50:1720–30.
[16] Abu-Nada E, Masoud Z, Oztop H, Campo A. Effect of nanofluid variable properties on natural convection in enclosures. Int J Thermal Sci 2010;49:479–91.
[17] Sebdani SM, Mahmoodi M, Hashemib SM. Effect of nanofluid variable properties on mixed convection in a square cavity. Int J Thermal Sci 2012;52:112–26.
[18] Natarajan E, Basak T, Roy S. Natural convection flows in a trapezoidal enclosure with uniform and non-uniform heating of bottom wall. Int J Heat Mass Transfer 2008;51:747–56.
[19] Basak T, Roy S, Singh A, Balakrishnan AR. Natural convection flows in porous trapezoidal enclosures with various inclination angles. Int J Heat Mass Transfer 2009;52:4612–23.
[20] Varol Y, Oztop HF, Pop I. Natural convection in right-angle porous trapezoidal enclosure partially cooled from inclined wall. Int Commun Heat Mass Transfer 2009;36:6–15.
[21] Saleh H, Roslan R, Hashim I. Natural convection heat transfer in a nanofluid-filled trapezoidal enclosure. Int J Heat Mass Transfer 2011;54:194–201.
[22] Nasrin R, Parvin S. Investigation of buoyancy-driven flow and heat transfer in a trapezoidal cavity filled with water–Cu nanofluid. Int Commun Heat Mass Transfer 2012;39:270–4.
[23] Bejan A. Entropy generation through heat and fluid flow. New York: Wiley; 1982.
[24] Mahmoudi AH, Shahi M, Talebi F. Entropy generation due to natural convection in a partialy open cavity with a thin heat source subjected to a nanofluid. Numer Heat Transfer A 2012;61:283–305.
[25] Shahi M, Mahmoudi AH, Honarbakhsh Raouf A. Entropy generation due to natural convection cooling of a nanofluid. Int Commun Heat Mass Transfer 2011;38:972–83.
[26] Singh PK, Anoop KB, Sundararajan T, Das SK. Entropy generation due to flow and heat transfer in nanofluids. Int J Heat Mass Transfer 2010;53:4757–67.
[27] Moghaddami M, Mohammadzade A, Esfehani SAV. Second law analysis of nanofluid flow. Energ Convers Manage 2011;52:1397–405.
[28] Esmaeilpour M, Abdollahzadeh M. Free convection and entropy generation of nanofluid inside an enclosure with different patterns of vertical wavy walls. Int J Thermal Sci 2012;52:127–36.
[29] Hamad MAA. Analytical solution of natural convection flow of a nanofluid over a linearly stretching sheet in the presence of magnetic field. Int Commun Heat Mass Transfer 2011;38:487–92.
[30] Ghasemi B, Aminossadati SM, Raisi A. Magnetic, field effect on natural convection in a nanofluid-filled square enclosure. Int J Thermal Sci 2011;50:1748–56.
[31] Nemati H, Farhadi M, Sedighi K, Ashorynejad HR, Fattahi E. Magnetic field effects on natural convection flow of nanofluid in a rectangular cavity using the Lattice Boltzmann model. Sci Iranica, in press. doi:10.1016/j.scient.2012.02.016.
[32] Hamad MAA, Pop I. Unsteady MHD free convection flow past a vertical permeable flat plate in a rotating frame of reference with constant heat source in a nanofluid. Heat Mass Transfer 2011;47:1517–24.
[33] Aminossadati SM, Raisi A, Ghasemi B. Effects of magnetic field on nanofluid forced convection in a partially heated microchannel. Int J Non-Linear Mech 2011;46:1373–82.
[34] Patel HE, Pradeep T, Sundararajan T, Dasgupta A, Dasgupta N, Das SK. A microconvection model for thermal conductivity of nanofluid. Pramana J. Phys 2005;65:863–9.
[35] Brinkman HC. The viscosity of concentrated suspensions and solutions. J. Chem. Phys. 1952;20:571–81.
[36] Maxwell JC. A treatise on electricity and magnetism. 2nd ed. Cambridge: Oxford University Press; 1904. p. 435–41.
[37] Ferziger JH, Peric M. Computational method for fluid dynamics. New York: Springer-Verlag; 1999.
[38] Patnkar SV. Numerical heat transfer and fluid flow. New York: Hemisphere; 1980.
[39] Asan H, Namli L. Laminar natural convection in a pitched roof of triangular cross-section: summer day boundary conditions. Energy Build 2000;33:69–73.
[40] Varol Y, Oztop HF, Koca A. Entropy production due to free convection in partially heated isosceles triangular enclosures. Appl Thermal Eng 2008;28:1502–13.
[41] Ghasemi B, Aminossadati SM. Brownian motion of nanoparticles in a triangular enclosure with natural convection. Int J Thermal Sci 2010;49:931–40.
[42] De Vahl Davis G. Natural convection of air in a square cavity a bench mark numerical solution. Int J Numer Method Fluids 1983;3:249–64.
[43] Venkatachalappa M, Subbaraya CK. Effect of a magnetic field on free convection in a rectangular enclosure. Int J Eng Sci 1995;33:1075–84.
[44] Jery AE, Hidouri N, Magherbi M, Brahim AB. Effect of an external oriented magnetic field on entropy generation in natural convection. Entropy 2010;12:1391–417.